HHS Public Access

Author manuscript

Nat Genet. Author manuscript; available in PMC 2019 January 16.

Published in final edited form as:

Nat Genet. 2018 August ; 50(8): 1086–1092. doi:10.1038/s41588-018-0170-4.

Krebs Cycle-Deficient Hereditary Cancer Syndromes are Defined by Homologous Recombination DNA Repair Defects

Parker L. Sulkowski[1,2], **Ranjini K. Sundaram**[1], **Sebastian Oeck**[1,3], **Christopher D. Corso**[1,4], **Yanfeng Liu**[1], **Seth Noorbakhsh**[1], **Monica Niger**[1,5], **Marta Boeke**[6], **Daiki Ueno**[6], **Aravind Nambiar Kalathil**[1], **Xun Bao**[7], **Jing Li**[7], **Brian Shuch**[6,*], **Ranjit S. Bindra**[1,8,*], and **Peter M. Glazer**[1,2,*]

[1]Department of Therapeutic Radiology, Yale University School of Medicine, New Haven, CT 06511

[2]Department of Genetics, Yale University School of Medicine, New Haven, CT 06511

[3]Institute of Cell Biology (Cancer Research), University of Duisburg-Essen, Medical School, Virchowstrasse 173, 45122 Essen, Germany

[4]Southeast Radiation Oncology and Levine Cancer Institute, Atrium Health, Charlotte, NC

[5]Medical Oncology Department, Fondazione IRCCS Istituto Nazionale dei Tumori, Milan, Italy

[6]Department of Urology, Yale University School of Medicine, New Haven, CT 06511

[7]Karmanos Cancer Institute, Wayne State University, Detroit MI 48201

[8]Department of Pathology, Yale University School of Medicine, New Haven, CT 06511

Abstract

The hereditary cancer syndromes, Hereditary Leiomyomatosis and Renal Cell Cancer (HLRCC) and Succinate Dehydrogenase-related Hereditary Paraganglioma and Pheochromocytoma (SDH PGL/PCC), are linked to germline loss-of-function mutations in the fumarate hydratase (FH) and succinate dehydrogenase (SDH) genes encoding Krebs cycle enzymes, leading to elevated levels of fumarate and succinate, respectively[1–3]. Here, we report that fumarate and succinate both suppress the homologous recombination (HR) DNA repair pathway required for the resolution of DNA double-strand breaks (DSBs) and for the maintenance of genomic integrity, rendering tumor cells vulnerable to synthetic lethal targeting with poly (ADP-ribose) polymerase (PARP) inhibitors. These results identify HLRCC and SDH PGL/PCC as familial DNA repair deficiency syndromes, providing a mechanistic basis to explain their cancer predisposition and pointing to a

*These authors jointly directed this work. Correspondence should be addressed to: Peter M. Glazer (peter.glazer@yale.edu), Ranjit S. Bindra (ranjit.bindra@yale.edu), or Brian Shuch (brian.shuch@yale.edu).

Author contributions.

P.L.S., R.K.S. S.O. and C.D.C. contributed to the experiments, scientific hypotheses, data analysis, and compiling of the manuscript. Y.L., S.N., M.N., M.B., D.U., A.K. X.B., J.L. contributed to the experiments and data analysis. P.M.G., R.S.B., and B.S. designed the experiments. P.L.S., B.S., R.S.B., and P.M.G. wrote the manuscript.

Competing financial interests.

The authors declare no competing interests.

new therapeutic approach for advanced HLRCC and SDH PGL/PCC, both incurable when metastatic.

Hereditary Leiomyomatosis and Renal Cell Cancer (HLRCC) and Hereditary Paraganglioma and Pheochromocytoma (SDH PGL/PCC) are autosomal dominant cancer predisposition syndromes characterized by the heterozygous inheritance of loss-of-function mutations in the *Fumarate Hydratase (FH)* gene or succinate dehydrogenases genes (*SDHA, SDHAF2, SDHB, SDHC* and *SDHD*), respectively[1–3]. Subsequent loss of heterozygosity (LOH) at these loci eliminates the remaining functional allele, resulting in excess accumulation of the respective metabolites: fumarate in the case of HLRCC, and succinate in SDH PGL/PCC[1,4]. Both metabolites are thought to have a driving role in these heredity cancer syndromes via inhibition of alpha-ketoglutarate (αKG) dependent dioxygenases[5]. Since these dioxygenases include enzymes that mediate histone demethylation or promote DNA demethylation, the associated oncogenesis has been attributed to disruption of normal epigenetic gene regulation. However, the mechanism by which these metabolites drive tumorigenesis is poorly understood. We recently reported that 2-hydroxyglutarate (2HG), an oncometabolite produced by the neomorphic activity of somatically mutated isocitrate dehydrogenase 1 and 2 (IDH1/2) enzymes in gliomas and other malignancies, causes homologous recombination (HR) deficiency due to the ability of 2HG to inhibit αKG-dependent enzymes[6]. Because fumarate and succinate can also inhibit these enzymes, we hypothesized that these metabolites might act in a manner analogous to 2HG. Here, we present the finding that the high levels of fumarate and succinate in HLRCC and SDH PGL/PCC, respectively, suppress HR via inhibition of two key lysine demethylases, KDM4A and KDM4B, thereby conferring a previously unsuspected vulnerability to inhibitors of poly (ADP-ribose) polymerase (PARP).

We profiled a collection of primary human HLRCC and SDH PGL/PCC tumor samples and corresponding control samples for fumarate and succinate production by liquid chromatography–mass spectrometry (LC/MS) (Fig. 1a,b) and for the presence of DNA double strand breaks (DSBs) by the neutral comet assay (Fig. 1a,b,c). We observed high levels of DNA DSBs in HLRCC samples (correlating with overproduction of fumarate) as well as in SDH PGL/PCC samples (producing high amounts of succinate). Quantification of the levels of the phosphorylated histone, γH2AX, another marker of DNA DSBs, by ELISA in formalin fixed, paraffin-embedded (FFPE) samples revealed high levels of γH2AX in HLRCC samples (Supplementary Fig. 1a), in keeping with reduced HR repair capacity.

Next, we sought to experimentally test the link between elevated DSBs and loss of *SDHB* or *FH* with the resultant metabolite overproduction. Using both a constitutive shRNA system and a doxycycline-inducible lentiviral shRNA system in the SV40-immortalized Yale University Normal Kidney 1 (YUNK1) cell line (derived from uninvolved cortical tissue from a nephrectomy specimen) and in HEK293FT kidney cells, we knocked down expression of *SDHB* or *FH*, yielding the expected increased production of succinate and fumarate, respectively (Fig. 2a,b,c and Supplementary Fig. 1b,c,d,e,f). With either SDHB or FH knockdown, we observed substantial increases in DSBs as measured by the comet assay (Fig. 2d and Supplementary Fig. 1g,h,i). We observed similar levels of elevated DSBs upon

knockdown of RAD51, BRCA1 and BRCA2 in YUNK1 and in HEK293FT cells, and upon BRCA2 homozygous knockout in DLD1 cells (Fig. 2d and Supplementary Fig. 1j,k,l). In addition, we found similar elevations in DNA DSBs in three patient-derived HLRCC cell lines, UOK 262[7] (*FH –/–*), UOK 268[8] (*FH p.His192Asp*) and NCCFH1[9] (*FH–/–*) (Fig. 2e), all three of which are deficient in FH activity (as confirmed by elevated levels of fumarate measured by LC/MS; Supplementary Fig. 1m). The elevated DSBs were suppressed in these lines upon complementation by transient expression of wild-type FH by plasmid transfection (Fig. 2e and Supplementary Fig. 1n), further supporting the link between fumarate and suppression of HR.

In addition to γH2AX foci, increased phosphorylated 53BP1 (p53BP1) nuclear foci are also markers of the cellular response to DNA DSBs, and HR-deficient cells show elevated levels of γH2AX and p53BP1 foci in the absence of exogenous DNA damage[6]. We found that shRNA knockdown of SDHB or FH resulted in high levels of γH2AX and p53BP1 foci, and that these foci levels were similar in magnitude to those seen in the context of siRNA knockdown of BRCA1, BRCA2 and RAD51, central factors in the HR pathway (Fig. 2f,g,h,i). High levels of these foci were also seen in UOK 262, UOK 268, and NCCFH1 cells (Fig. 2h,i).

To directly test for DNA DSB repair deficiency, we employed two different luciferase-based DNA repair assays[6,10–13], that can report either HR or non-homologous end-joining (NHEJ) activity (Fig. 2j). These assays can assess the relative differences in pathway specific DNA DSB repair activity across cell lines (Supplementary Fig. 1o). We noted suppression of the HR pathway, along with a slight increase in the NHEJ pathway, as a function of both SDHB or FH knockdown (Fig. 2k,l and Supplementary Fig 1p) and in the patient-derived HLRCC cell lines (Fig. 2m). Complementation by expression of WT *FH* rescued HR function (Fig. 2m). Next, we sought to further evaluate the extent of the HR suppression using the well-established DR-GFP assay in U2OS cells, a chromosomal reporter assay for HR that is widely used as a benchmark assay in the DNA repair field[6,14,15](Fig. 2n). We found that siRNAs targeting SDHB or FH resulted in substantial suppression of HR and that this suppression was similar in magnitude to that seen with siRNAs targeting key HR proteins including BRCA1, BRCA2, and RAD51 (Fig. 2o and Supplementary Fig. 2q). Another measure of HR capacity is the formation of RAD51 foci in response to DNA damage. We observed that YUNK1 and HEK293FT cells with SDHB or FH knockdown have a deficiency in RAD51 foci formation after treatment with ionizing radiation (IR) consistent with reduced HR (Fig. 2p,q and Supplementary Fig. 2r).

We next tested if elevated levels of fumarate and succinate, themselves, are sufficient to drive the HR deficiency associated with SDHB or FH loss. We found that addition of the metabolites and/or cell permeable versions thereof (succinate, monoethyl-succinate, dimethyl-succinate, monoethyl-fumarate and dimethyl-fumarate) to the cell culture medium was sufficient to suppress HR in a dose-dependent manner as measured using the DR-GFP assay (Fig. 3a). The metabolites alone were sufficient to suppress HR in YUNK1 cells as measured by the luciferase-based HR reporter assay (Fig. 3b). Metabolite treatment of the YUNK1 cells also induced elevated DNA DSBs in the comet assay (Fig. 3c,d and Supplementary Fig. 2a,b,c). Similar effects of the metabolites were seen in other cell lines

(Supplementary Fig. 2d,e,f,g,h). Increases in γH2AX and p53BP1 foci were also produced by addition of succinate or dimethyl-fumarate to the cell culture media in the HEK293FT cells (Fig. 3e,f,g) and YUNK1 cells (Supplementary Fig. 2i,j,k,l). In a demonstration of epistasis, exogenous fumarate and succinate had no further effect on the levels of DNA DSBs in the *FH*-deficient HLRCC cells, UOK 262 and UOK 268, that already overproduce fumarate because of functional FH loss (Fig. 3h).

Mechanistically, fumarate and succinate have similar structure and are known to converge in function by competitively inhibiting αKG dependent dioxygenases, including the lysine demethylases, KDM4A and KDM4B, which we and others have recently shown to be key regulators of DNA repair[6,16,17]. To directly test for the predicted suppression of KDM4A and KDM4B activity, we performed western blots to measure the levels of tri-methylated histone 3 lysine 36 (H3K36me3) and tri-methylated histone 3 lysine 9 (H3K9me3), known targets for demethylation by KDM4A and B. We found that H3K36me3 and H3K9me3 levels were elevated in human tumors with SDHB or FH deficiency (Fig. 3i), in patient-derived HLRCC cell lines (UOK 262 and UOK 268) (Supplementary Fig. 3a), in YUNK1 and HEK293FT cells with SDHB or FH knockdown (Supplementary Fig. 3a,b,c), and in xenograft tumors formed by HEK293FT cells with SDHB knockdown (Supplementary Fig. 3d), compared to respective controls. We also observed a dose-dependent increase in H3K36me3 and H3K9me3 levels upon treatment of YUNK1 cells with increasing doses of fumarate and succinate (Supplementary Fig. 3e,f). These findings all provide functional evidence of KDM4A and B inhibition by elevated levels of succinate and fumarate.

Next, we sought to test the hypothesis that the HR suppression conferred by fumarate and succinate is mediated through this inhibition of KDM4A/B. By forced expression of KDM4A or KDM4B, we rescued the elevated DSB phenotype (as measured by comet assay) of the two patient-derived HLRCC cell lines, UOK 262 and UOK 268, as well as the comet phenotype in YUNK1 induced by exogenous fumarate and succinate (Fig. 3j,k). There was no effect seen when KDM4C was over-expressed, even though KDM4C is a member of the same JMJD2 family as KDM4A and B and shares substantial homology with them[18], showing the specificity for the KDM4A/B proteins (Fig. 3j). Further, the addition of αKG to the cells (to compete out the fumarate) also rescued the phenotype in the FH deficient cells (Fig. 3j) as well as the HR defect induced by succinate or fumarate, as measured in the DR-GFP assay (Fig. 3l).

We next hypothesized that the HR defect conferred by SDH or FH deficiency would render cells sensitive to DNA damaging agents. To test this possibility, we performed clonogenic survival assays which showed that upon SDHB or FH knockdown cells have substantially reduced survival in response to IR, mitomycin C, cisplatin, and etoposide compared to the control shRNA (Supplementary Fig. 4a, b,c,d).

Clinically, an emerging strategy in the treatment of HR deficient cancers is the use of PARP inhibitors (PARPi), which recently have been approved by the FDA for use in patients BRCA1/2 deficient cancers[19,20]. We therefore tested the effects of fumarate and succinate on PARPi sensitivity. We observed that knockdown of SDHB and FH as well as addition of exogenous dimethyl-fumarate or succinate to the culture media induced dramatic sensitivity

to the PARP inhibitors, olaparib and BMN-673 (Fig. 4a,b and Supplementary Figs. 4 e,f,g,h,i). The FH-deficient HLRCC cell line, UOK 262, was markedly more sensitive to the PARPi, BMN-673 (Fig. 4c) (and to mitomycin C; Supplementary Fig. 4j) than other cell lines of renal origin that are FH-proficient. Exogenously added succinate and fumarate analogs also strongly sensitized HeLa cells to PARPi as well (Supplementary Fig. 4k,l).

To test for this succinate and fumarate-induced PARPi sensitivity in tumors *in vivo*, we assayed the effect of the PARP inhibitor, BMN-673, on the growth of tumor xenografts formed in immune deficient mice by HEK293FT cells expressing either a non-targeting control shRNA (shCTRL), an shRNA to SDHB (shSDHB), or an shRNA to FH (shFH) (knockdown is shown in Supplementary Fig. 1g,h). (HEK293FT is a tumorigenic cell line transformed by expression of SV40 Large T antigen). We observed that BMN-673 significantly inhibited the growth of both the SDHB-deficient and FH-deficient tumors in two separate sets of *in vivo* efficacy studies. In one set, mice were treated beginning four days after tumor cell implantation, showing robust suppression of tumor growth by the PARPi compared to the vehicle control in the shSDHB and shFH tumors with no effect in the shCTRL tumors (Fig. 4d,e,f). In the second set, the mice were treated after the tumors had grown to a palpable size (95–150 mm^3) (Fig. 4g,h,i). Again, BMN-673 inhibited the growth of the SDH-deficient and FH-deficient tumors (Fig. 4g,h), but there was no growth inhibition relative to vehicle control in xenografts formed from the HEK293FT cells expressing the control shCTRL (Fig. 4i). Quantification of intra-tumoral BMN-673 levels 24 h after treatment by LC/MS showed no significant difference in drug levels between shSDHB and shCTRL HEK293FT tumors (Fig. 4j). In keeping with this, levels of poly-ADP-ribose (PAR) modification of cellular proteins as measured by ELISA (Fig. 4k) and by western blot (Supplementary Fig. 5a,b) were reduced to the same extent 24 h post BMN-673 treatment in the SDHB knockdown tumors as in the shCTRL tumors.

Next, we conducted a third *in vivo* efficacy study using tumors formed from the UOK 262 cells, that, as discussed above, are an HLRCC patient-derived cell line deficient in FH. We observed a significant growth delay with PARPi treatment administered daily to the mice beginning 4 days after implantation and continued on a long-term basis for 180 days (Fig. 4l). In a fourth *in vivo* experiment, we treated mice with BMN-673 or with vehicle control beginning when the UOK 262 xenografts had reached an average size of 250 mm^3 (after approximately 150 days of pre-treatment growth). Again, we found that the PARPi treatment (but not vehicle control) resulted in a substantial growth delay in the FH-deficient tumors (Fig. 4m). Together, these four *in vivo* tumor efficacy studies consistently show that PARPi treatment suppresses the growth of SDH- or FH- deficient tumors in mice.

The results presented here demonstrate that the metabolites overproduced in the hereditary cancer syndromes, HLRCC and SDH PGL/PCC, compromise HR DNA repair (Fig. 4n). This finding identifies decreased DNA repair as a key oncogenic mechanism in these diseases much like the familial breast and ovarian cancer predisposition syndromes linked to the BRCA1/2 genes. In addition, our finding that succinate and fumarate render tumor cells highly susceptible to synthetic lethal targeting with PARP inhibitors provides a novel therapeutic strategy that could potentially be translated into the clinic for these otherwise difficult to treat malignancies.

Online Methods

Western Blot analyses

Western blot analysis of protein levels was conducted by loading 30 μg of whole cell lysate onto a 4–20% polyacrylamide gel. Total protein was transferred to a nitrocellulose membrane. After blocking with 5% milk, membranes were incubated with primary antibodies. Antibodies used were: Rabbit monoclonal anti-Fumarase (D9C5, Cell Signaling Technologies) 1:1000 in 5% BSA, mouse monoclonal anti-SDHB (21A11AE7, Abcam) 1:1000 in % 5 milk, mouse monoclonal anti-Vinculin (SPM227, Abcam) 1:1000 in 5% milk, rabbit polyclonal anti-Histone 3 Lysine 36 trimethyl (9050, Abcam) 1:500 in 5% BSA, anti-Histone 3 Lysine 9 trimethyl (D4W1U, Cell Signaling Technologies) 1:1000 in 5% BSA, mouse monoclonal anti-Beta Actin (60008, Protein Tech) 1:5000 5% milk, rabbit Polyclonal anti-Histone H3 (ab1791, Abcam 1:5000 5% BSA), rabbit Polyclonal anti-PAR (4336-BPC-100, Trevigen) 1:5000 5% BSA, mouse monoclonal anti-GAPDH (60004 Protein Tech) 1:5000 5% milk, mouse monoclonal anti-BRCA2 (ab1, Millipore, 1:1000 5% Milk), mouse monoclonal anti-BRCA1 (D-9, Santa Cruz, 1:200 5% milk), mouse monoclonal anti-RAD51(14B4 Novus bio, 1:1000 5% milk). Patient sample blots were reprobed. Reprobed blots were stripped with Restore Plus Stripping Buffer (Thermo Fischer) and re-blocked with 5% milk prior to reprobing. Blots were tested to ensure all residual detection reagents were removed. Dual Color Precision Plus Protein standard was used as a molecular weight standard for western blots.

Cell Culture

YUNK1 cells were generated in culture from uninvolved cortical renal tissue from a patient undergoing a radical nephrectomy for kidney cancer. This cell line was grown in DMEM with 10% FBS and was capable of 10 passages before senescence. YUNK1 was immortalized with a lentiviral vector containing SV40 Large T antigen (Addgene plasmid #22298). Lentiviral production was performed using HEK293FT (ATCC) using plasmids pMDLg/pRRE, pRSV-Rev, pCMV-VSG-G (Addgene #12251, 12253, and 8454) similar to previously described methods.[1] YUNK1 cells were maintained in DMEM+10% FBS+1% Pen/Strep. HEK293FT cells (ATCC) were maintained in DMEM+10% FBS+1% Pen/Strep. After lentiviral infections with TRIPZ-shRNA or GIPZ lentiviruses, cells were maintained in DMEM+10%FBS+1% Pen/Strep + 2μg/mL Puromycin. For dox inducible shRNAs, expression was induced with 2μg/mL doxycycline. Doxycycline induced knockdown was monitored by western blot as well as by RFP fluorescence from the internal and dox-inducible reporter on the TRIPZ construct. U2OS DR-GFP cells have been previously described[15] and were maintained in DMEM+10% FBS+1% Pen/Strep. UOK 262 and UOK 268 HLRCC cells are previously described[7,8]. They were obtained courtesy of W.M. Linehan and were maintained in DMEM+10% FBS+1% Pen/Strep + 1mM Sodium-Pyruvate. NCCFH1 cells have been previously described[9] were maintained in DMEM+10% FBS+1% Pen/Strep + 1mM Sodium-Pyruvate. Hela cells (ATCC), RCC4 (ATCC) and 786-O (ATCC) were maintained in DMEM+10% FBS+1% Pen/Strep.

Tumor Samples

All tumor samples were de-identified. The Sample bank was approved by the Yale Human Investigation Committee (HIC) and all subjects were consented. There are no identifiable images.

Chemicals

Succinate (S9512, Sigma), monoethyl-succinate (475505, Sigma), dimethyl-succinate (112755, Sigma), monoethyl-fumarate (128422, Sigma), dimethyl-fumarate (242926,Sigma), and dimethyl-alpha-ketoglutarate (349631, Sigma) were obtained from Sigma Aldrich.

shRNA

Doxycycline-inducible shRNA knockdowns were made using TRIPZ doxycycline-inducible shRNA lentiviruses available from Ge Dharmacon. Lentiviral particles were produced using plasmids pMDLg/pRRE, pRSV-Rev, pCMV-VSG-G (Addgene #12251, 12253, and 8454). The TRIPZ shRNA clones used were as follows, shFH#1: Ge Dharmacon, V3THS_324846, TRIPZ shFH#2: Ge Dharmacon, V3THS_324847. TRIPZ shSDHB#1: Ge Dharmacon, V3THS_346327, TRIPZ shSDHB#2: Ge Dharmacon, V3THS_347328, and TRIPZ non-targeting control (RHS4743, Ge Dharmacon). Pooled populations and single cell clones were selected with 2 μg/mL Puromycin and maintained in selective media. Single cell clones were derived by limiting dilution. shRNA expression was induced with 1 μg/mL Doxycline for 4 days before starting an assay, and repression of the target proteins was routinely monitored by western blot. Constitutive shRNA knockdown shRNA lentivirus were produced using identical protocols using the GIPZ lentiviral constructs, for shFH#1: Ge Dharmacon, V2LHS_83495, shFH#2 Ge Dharmacon, V3LHS_403312, shSDHB#1 Ge Dharmacon, V3LHS_346327, shSDHB#2 Ge Dharmacon, V3LHS_346329 and GIPZ non-targeting control (RHS4348, Ge Dharmacon). Cells were selected in 2 μg/mL Puromycin and maintained in selective media and clones were isolated by limiting dilution in selective media.

Neutral comet assays

Neutral comet assays were performed as previously described[6]. Patient tumor samples were processed one at a time, diced with a razor blade on ice to dissociate the cells in cold PBS, counted and suspended in low-melt agarose at a concentration of 2000 cells per assay. Upon solidification of the agarose, the cells were immediately lysed and the neutral comet assay was performed as previously described[6]. Neutral comet assays on cell line samples were performed as previously described[6]. For doxycycline-inducible shRNA of FH and SDHB, the assays were performed 5 days after induction of shRNA with 2 μg/mL Doxycycline. For plasmid transfection assays, 1×10^5 cells per well were seeded in a 12-well dish and allowed to attach overnight. The next day the cells were transfected with 1 μg of pCMV-FH (Origene), pCMV-HA-JMJ2A (KDM4A) (Addgene), pCMV-HA- JMJ2B (KDM4B) (Addgene), or pCMV-HA-GASC1 (KDM4C) (Addgene) using 1 μL of Lipofectamine 3000 and 1 μL of p3000 reagent. 48h later cells were collected on ice, suspended in PBS, and then adjusted to a concentration of 2000 cells per assay in low melt agarose. For assays following

treatment with exogenous metabolites, these were added 24h before performing the neutral comet assay. Data are presented as means of three biological replicates ± SEM. Replicates reflect independent cultures for in vitro assays. For analysis for patient samples, 3 replicates were performed on each patient tissue sample.

siRNA

siRNA transfections were carried out with Dharmafect 2 (GE Dharmacon) per manufacturers protocol with final siRNA concentration at 20 nM for all assays. siRNAs used were ON-TARGET Plus siRNA targeting BRCA1 (GE Dharmacon, L-003461), RAD51 (GE Dharmacon, L-003530), BRCA2(L-003462, GE Dharmacon), SDHB (GE Dharmacon, L-011773), FH (L-009512, GE Dharmacon) and the ON-TARGET Plus siRNA non-targeting control (GE Dharmacon, D-001810)

γH2AX ELISA

FFPE samples were collected as a 10 μM slice off the tissue block. Samples were deparaffinized with 3 washes in 1 mL xylene. Samples were then washed 3 times in 100 % Ethanol, followed by 3 washes in 85% Ethanol and 3 washes in 70% Ethanol. Samples were then incubated in extraction buffer (20 mM TRIS pH 8.8, 100 mM DTT, 2% SDS) and incubated at 100 °C for 20 min, followed by a 2 h incubation at 60 °C. Protein extracts were quantified using the DC Protein Assay (Bio Rad) and then stored at −20 °C. The γH2AX ELISA assay was performed using the γH2AX Pharmacodynamic Assay Kit per manufacturers protocol, using an input of 2 μg protein per replicate. Data are presented as means of three biological replicates ± SEM.

Luciferase-based reporter assays for homology-directed repair and non-homologous end-joining

These assays were previously described[6]. Briefly, the HR luciferase reporter construct was generated by cloning an inactivating I–SceI recognition site into the BstBI site 56 amino acids into the firefly luciferase gene in the gWIZ.Luciferase vector (Genlantis) and cloning a promoterless copy of the firefly luciferase ORF 700 base pairs downstream in reverse orientation as a donor template for HR. A DSB in the firefly luciferase gene is induced by I–SceI digestion and confirmed by electrophoresis. Linearized plasmid is then transfected into cells to measure HR as a function of luciferase activity (firefly luciferase activity can only be restored by HR, which removes the inactivating I–SceI site). To assay NHEJ, a Hind III–mediated DSB was generated between the promoter and the coding region of the firefly luciferase gene in the pGL3-Control Vector (Promega) and confirmed by electrophoresis. After transfection of linearized plasmid, repair of the DSB by NHEJ restore firefly luciferase activity. All reporter assays were performed in 12-well format by seeding 1×10^5 cells per well 24 hours before transfection and transfecting 1 μg of reporter or positive control vector and 50 ng of *Renilla* luciferase vector (as a transfection control) per well. For HR, cells were analyzed 48 hours after reporter transfection, and for NHEJ, cells were analyzed 24 hours after reporter transfection. Luciferase activity was measured using the Dual-Luciferase Reporter Assay System (Promega) for all samples and normalized to *Renilla* luciferase signal to control for transfection efficiency, to the positive control luciferase expression

vector: gWIZ.luciferase for HR or pGl3-Control for NHEJ. Data are presented as means of three biological replicates ± SEM.

U2OS DR-GFP assays

U2OS DR-GFP assays were performed as previously described[15,6]. siRNAs were transfected to a final concentration of 20nM, and cells were assayed 96h after siRNA transfection. Metabolites were added to the cells at indicated concentration 24h before performing the assay.

Clonogenic survival assay

After 5 days of Doxycycline exposure for the shRNA models, cells in culture were irradiated at varying doses of IR. Four hours after irradiation, they were trypsinized, washed, counted, and seeded in six-well plates in triplicate at threefold dilutions, ranging from 1200 to 300 cells per well. For drug treatments, cells were seeded 24 hours before addition of the drug. PARP inhibitors were added and left on the cells for the duration of the assay. Cisplatin was a 24h treatment, and MMC and Etoposide were 1 h treatments. For assays that included treatment with exogenous metabolites, these were added 24 h before the drug treatment. Plates were incubated for 10–14 days until colonies formed. Colonies were fixed with 2% formaldehyde, then stained with crystal violet and quantified.

Immunofluorescence and Foci Assays

Primary antibodies: γH2AX antibody mouse (1:400; #05-636; EMD Millipore), phospho-53BP1 rabbit (1:300; #2675; Cell Signaling Technology), Rad51 antibody rabbit (1:300; #PC130-100; EMD Millipore). Secondary antibodies: anti-mouse AF Plus 488, anti-mouse AF Plus 647, anti-rabbit AF Plus 488, anti-rabbit AF Plus 647 (1:400; #A32723, #A32728, #A32731, #A32733; Thermo Fisher Scientific). Cells were seeded in chamber slides. Subsequently, cells were fixed and permeabilized in 3% PFA/0.2% Triton-X100/2% sucrose for 20 min and blocked with 10% bovine serum albumin in PBS overnight at 4°C. Proteins were stained overnight at 4°C with primary antibodies diluted in blocking solution. Upon three times of washing with 0.5% Triton-X100 in PBS, samples were incubated with secondary antibodies for 90 min at RT. DNA was stained with DAPI (2.5 μg/mL; #1816957; Thermo Scientific Inc) for 20 min at RT. After staining and 3 times washing, chambers were removed from the slides and the slides were covered with coverslips using DAKO Fluorescence Mounting Medium (#S3023; Dako NA Inc.). Images were analyzed with a Nikon Eclipse Ti fluorescence microscope with a Plan Apo 60X/1.40 Oil DIC h objective, a CSU-W1 confocal scanning unit with a iXon Ultra camera (Andor Technology), MLC 400B laser unit (Agilent Technologies) and NIS Elements 4.30 software (Nikon Corporation). Foci were analyzed with the Focinator v2-21 software as previously described[21]. RAD51 foci analysis plus radiation was performed 4 h after 2 Gy IR, cells with greater than 20 foci per nucleus were considered RAD51 positive. For γH2AX greater than 15 foci per nucleus were considered foci positive cells and for p53BP1 analysis greater than 5 foci per nucleus were considered foci positive cells.

LC-MS/MS analysis

The concentrations of succinate and fumarate in frozen tissue and cell samples were determined using a validated liquid chromatography-tandem mass spectrometry (LC-MS/MS) method, as described below. The calibration curve was prepared in distilled water, with the concentration range of 0.002 – 10 μM for succinate and 0.02 – 100 μM for fumarate. The intra- and inter-day precision and accuracy of the quality control samples met the generally accepted criterial for bioanalytical methods (i.e., <15%). *Sample preparation.* Tissue homogenate was prepared by adding 100 μL of distilled water to a weighted tissue sample (~ 20 mg) followed by homogenization using a Precellys® homogenizer (at 6500 RPM for two 20 seconds with 5 seconds pause). Cell homogenate was prepared by adding 500 μL water into cell pellet (~ 5 million cells) followed by sonication. Into tissue or cell homogenate (original or 20-fold diluted sample), the stable isotope labeled internal standards, D_6-succinate and 1,4-$^{13}C_2$, 2,3-D_2-fumarate, were added and followed by vortexed-mixing. Then, 60 μL was taken and protein precipitated by adding 240 μL of ice-cold methanol. The supernatant was transferred to a 2-mL Eppendorf tube; 0.1 mL of ice-cold 80% methanol was added to the precipitated pellet followed by vortex-mixing and centrifugation (at 10,000 rpm, 4°C for 10 min). The supernatants from two extractions were combined, and dried-down using a CentriVap® Refrigerated Centrifugal Concentrator (Kansas City, MO) at 10°C. The residue was reconstituted in 60 μL distilled water followed by vortex-mixing and centrifugation, and 5 μL of the supernatant was injected into the LC-MS/MS system. *LC-MS/MS analysis.* All LC-MS/MS analyses were performed on an AB SCIEX (Foster City, CA) QTRAP 6500 system, which consists of an enhanced high-performance hybrid triple quadrupole / linear ion trap mass spectrometer, interfaced with a SHIMADZU (Kyoto, Japan) Nexera ultra-high-performance liquid chromatography (UHPLC) system. Chromatographic separation was achieved on a Synergi RP column (2.0 mm × 150 mm, 4 μm) under a gradient elution consisting of mobile phase A (0.03% formic acid in water) and mobile phase B (0.03% formic acid in acetonitrile), at a flow rate of 0.25 mL/min. Succinate, fumarate, and their respective internal standards were monitored under the negative electrospray ionization mode at the mass transitions of 117.0 > 73.0, 114.9 > 71.0, 121.0 > 76.9, and 119.0 > 74.0, respectively. Analyst® 1.6 software was used for system control and data acquisition and MultiQuant® 3.0 software was used for data processing and quantitation.

In vivo efficacy studies: HEK293FT xenografts

Female athymic nu/nu mice (Hsd:Athymic Nude-Foxn1nu, Envigo) were used for all in vivo xenograft studies. The authors confirm that all animal experiments were performed in accordance with relevant guidelines and regulations. All studies were approved by the Yale University Institutional Animal Care and Use Committee. Mice were quarantined for at least 1 week before experimental manipulation. Tumors were formed using shRNA-expressing versions of the tumorigenic human embryonic kidney cell-derived line, HEK293FT. HEK293FT is a subline of HEK293 cells that has been transformed by expression of SV40 Large T-antigen. TRIPZ-shSDHB, shFH, or shCTRL (non-targeted control) expressing HEK293FT cells were implanted subcutaneously (5×10^6 cells in 0.1 cc PBS) in the right flank of nude mice. Two efficacy studies were conducted. In one, mice were randomized into treatment and non-treated groups (10 mice/group) at day 3, with treatment initiation 4

days post implant. In a second independent in vivo efficacy study, mice were injected as above with 10 mice per group, and treatment was started only once the tumor volumes reached 95–150mm. For both studies, mice were visually observed daily and tumors were measured three times per week by calipers to determine tumor volume using the formula: Volume = L × W × W × 0.532. Mice were fed with a grain based rodent diet containing Doxycycline at 200 mg/kg (Bioserv, Catalog # S3888). BMN-673 was solubilized in DMSO and diluted with PBS containing 10% dimethylacetamide (Sigma-Aldrich) and 6% Solutol (Sigma). BMN-673 (0.5 mg/kg, 0.2 cc), or vehicle (0.2 cc) was administered by oral gavage once daily for the duration of the experiment. Mean (geometric) tumor volume (mm^3) was plotted over time to monitor tumor growth. P-values were determined by.

In vivo efficacy studies: UOK 262 xenografts

Female athymic nu/nu mice (Hsd:Athymic Nude-Foxn1nu, Envigo) were used for all in vivo xenograft studies. The authors confirm that all animal experiments were performed in accordance with relevant guidelines and regulations. Institutional Animal Care and Use All studies were approved by the Yale University Institutional Animal Care and Use Committee. Mice were quarantined for at least 1 week before experimental manipulation. UOK 262 cells were implanted subcutaneously using 5×10^6 cells in 0.1 cc PBS mixed with 0.1 cc of Corning Matrigel Matrix (Cat. No. 354234) per animal. Mice were randomized at day 3 day into two groups (n=10/group). Olaparib (Selleckchem) was solubilized in DMSO and diluted with 10% (w/v) 2-hydroxy-propyl-beta-cyclodextrin (Sigma) to obtain the desired concentration and delivered via intraperitoneal injection (50 mg/kg) once daily, five days per week. In a second, UOK 262 in vivo efficacy study, mice were randomized into treatment and control groups (n=6 per group) after the volume reached 250mm. The control group received the vehicle and the other group received BMN-673 (0.5mg/kg, 0.2cc) gavage administered daily.

LC/MS analysis of intratumoral BMN-673

Human embryonic kidney cells TRIPZ-shSDHB or shCTRL (non-targeted control) subcutaneously (5×10^6 cells in 0.1 cc PBS) in both flanks. Tumors developed with mice on a rodent diet including doxycycline just as in the in *vivo* efficacy studies. Once tumors were at $80mm^3$ mice were gavaged with BMN-673 at 1 or 10mg/kg or vehicle. Tumors were collected 24 hours later for and frozen at −80 °C. The concentrations of BMN-673 in tumor samples were determined using liquid chromatography with tandem mass spectrometry (LC-MS/MS). In brief, an aliquot (30 μL) tumor homogenate was protein precipitated with 3 volumes of methanol, and 5 μL of supernatant was injected into the LC-MS/MS system. LC-MS/MS analyses were performed on a Waters LC-MS/MS system consisting a Waters AQUITY UPLC system coupled with a TQ-XS triple quadrupole mass spectrometer (Milford, MA, USA). Chromatographic separation was achieved on an XBridge C18 column (2.1 × 50 mm, 3.5 μm) using a gradient elution consisting of acetonitrile and 0.1% formic acid in water, at a flow rate of 0.4 mL/min. BMN673 was monitored using the positive electrospray ionization mode at the most sensitive and specific mass transition, m/z 381.0 > 228.8. The linear calibration curve was established at BMN673 concentration range of 5 – 5000 nM in mouse serum. The precision and accuracy of quality control samples were within generally acceptable criteria for bioanalytical methods.

Poly-ADP-Ribose ELISA

Poly-ADP-Ribose ELISA was performed per manufacturer's protocol using the PARP in vivo Pharmacodynamic Assay II Kit (Trevigen). 2 μg of protein input was used per replicate and luminescence reading were converted to pg PAR/μg protein using a standard curve.

Statistics and Reproducibility

Data are means ± SEM and compared using two-sided *t*-test, or ANOVA with repeated measures when appropriate. All t-tests were two-sided. Statistical analyses were carried out using GraphPad Prism and Stata software. Replicates were defined as individual cultures for all in vitro assays and statistics were performed on measurements from independent cultures. For in vivo assays replicates were defined as individual mice harboring a xenograft tumor.

Reporting Summary

Further information on experimental design is available in the Nature Research Reporting Summary linked to this article.

Data availability

The data that support the findings of this study are available from the corresponding author upon reasonable request.

Supplementary Material

Refer to Web version on PubMed Central for supplementary material.

Acknowledgments

We thank Denise Hegan and Amrit Dhawan for their help. This work was supported by the NIH (R01ES005775 and R35CA197574 to P.M.G. and R01CA215453 to R.S.B) and by the American Cancer Society (research scholar grant to R.S.B.). P.L.S. was supported by the NIH National Institute of General Medical Sciences training grant T32GM007223.

References

1. Merino MJ, Torres-Cabala C, Pinto P, Linehan WM. The morphologic spectrum of kidney tumors in hereditary leiomyomatosis and renal cell carcinoma (HLRCC) syndrome. The American journal of surgical pathology. 2007; 31:1578–1585. [PubMed: 17895761]
2. Buffet A, et al. A decade (2001–2010) of genetic testing for pheochromocytoma and paraganglioma. Hormone and Metabolic Research. 2012; 44:359–366. [PubMed: 22517557]
3. Schimke RN, Collins DL, Stolle CA. Paraganglioma, neuroblastoma, and a SDHB mutation: Resolution of a 30-year-old mystery. American Journal of Medical Genetics Part A. 2010; 152:1531–1535.
4. Gimenez-Roqueplo A-P, Dahia P, Robledo M. An update on the genetics of paraganglioma, pheochromocytoma, and associated hereditary syndromes. Hormone and Metabolic Research. 2012; 44:328–333. [PubMed: 22328163]
5. Xiao M, et al. Inhibition of α-KG-dependent histone and DNA demethylases by fumarate and succinate that are accumulated in mutations of FH and SDH tumor suppressors. Genes & development. 2012; 26:1326–1338. [PubMed: 22677546]
6. Sulkowski PL, et al. 2-Hydroxyglutarate produced by neomorphic IDH mutations suppresses homologous recombination and induces PARP inhibitor sensitivity. Science translational medicine. 2017; 9:eaal2463. [PubMed: 28148839]

7. Yang Y, et al. UOK 262 cell line, fumarate hydratase deficient (FH−/FH−) hereditary leiomyomatosis renal cell carcinoma: in vitro and in vivo model of an aberrant energy metabolic pathway in human cancer. Cancer genetics and cytogenetics. 2010; 196:45–55. [PubMed: 19963135]
8. Yang Y, et al. A novel fumarate hydratase-deficient HLRCC kidney cancer cell line, UOK268: a model of the Warburg effect in cancer. Cancer genetics. 2012; 205:377–390. [PubMed: 22867999]
9. Perrier-Trudova V, et al. Fumarate Hydratase-deficient Cell Line NCCFH1 as a New In Vitro Model of Hereditary Papillary Renal Cell Carcinoma Type 2. Anticancer Res. 2015; 35:6639–53. [PubMed: 26637880]
10. Czochor JR, Sulkowski P, Glazer PM. miR-155 Overexpression Promotes Genomic Instability by Reducing High-fidelity Polymerase Delta Expression and Activating Error-Prone DSB Repair. Molecular Cancer Research. 2016; 14:363–373. [PubMed: 26850462]
11. Bahal R, et al. In vivo correction of anaemia in β-thalassemic mice by γPNA-mediated gene editing with nanoparticle delivery. Nature Communications. 2016; 7
12. Scanlon SE, Sulkowski PL, Glazer PM. Suppression of homology-dependent DNA double-strand break repair induces PARP inhibitor sensitivity in VHL-deficient human renal cell carcinoma. AACR. 2017
13. Scanlon SE, Scanlon CD, Hegan DC, Sulkowski PL, Glazer PM. Nickel induces transcriptional down-regulation of DNA repair pathways in tumorigenic and non-tumorigenic lung cells. Carcinogenesis. 2017; 38:627–637. [PubMed: 28472268]
14. Pierce AJ, Johnson RD, Thompson LH, Jasin M. XRCC3 promotes homology-directed repair of DNA damage in mammalian cells. Genes Dev. 1999; 13:2633–8. [PubMed: 10541549]
15. Bindra RS, Goglia AG, Jasin M, Powell SN. Development of an assay to measure mutagenic non-homologous end-joining repair activity in mammalian cells. Nucleic Acids Res. 2013; 41:e115. [PubMed: 23585275]
16. Young LC, McDonald DW, Hendzel MJ. Kdm4b histone demethylase is a DNA damage response protein and confers a survival advantage following γ-irradiation. Journal of Biological Chemistry. 2013; 288:21376–21388. [PubMed: 23744078]
17. Mallette FA, et al. RNF8- and RNF168-dependent degradation of KDM4A/JMJD2A triggers 53BP1 recruitment to DNA damage sites. The EMBO journal. 2012; 31:1865–1878. [PubMed: 22373579]
18. Berry WL, Janknecht R. KDM4/JMJD2 histone demethylases: epigenetic regulators in cancer cells. Cancer Res. 2013; 73:2936–42. [PubMed: 23644528]
19. Helleday T. The underlying mechanism for the PARP and BRCA synthetic lethality: clearing up the misunderstandings. Molecular oncology. 2011; 5:387–393. [PubMed: 21821475]
20. Lord CJ, Ashworth A. BRCAness revisited. Nature Reviews. Cancer. 2016; 16:110–120. [PubMed: 26775620]
21. Oeck S, et al. The Focinator v2-0–Graphical Interface, Four Channels, Colocalization Analysis and Cell Phase Identification. Radiation Research. 2017

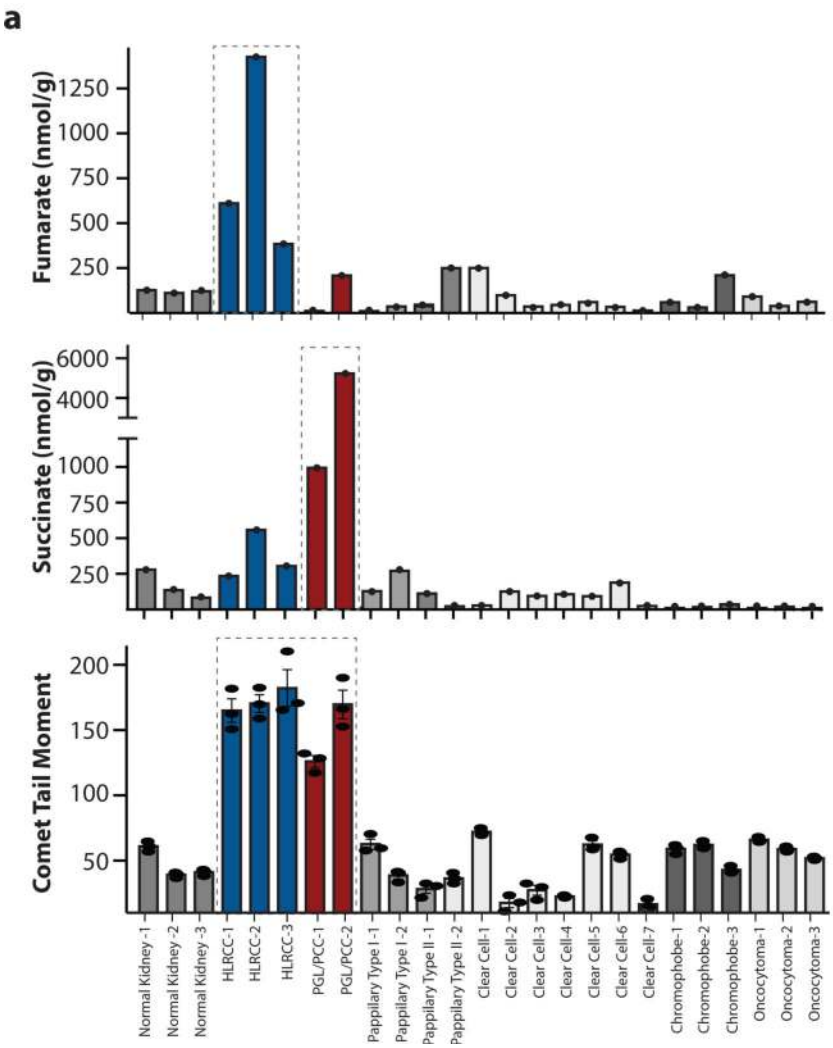

b

Specimen	Size	Grade	T stage	M Stage
Normal Kidney-1	-	-	-	-
Normal Kidney-2	-	-	-	-
Normal Kidney-3	-	-	-	-
HLRCC-1 Renal Lymph Node	9	3	T3a	M1
HLRCC-2 Renal Metastases	10	2	T2	M1
HLRCC-3	16	3	T4	M1
SDHB Head and Neck PGL-1	2	-	-	M0
SDHB Abdominal PGL-2	9.5	-	-	M0
Papillary RCC, Type 1 -1	13	2	T3a	M0
Papillary RCC, Type 1 -2	2.1	2	T1a	M0
Papillary RCC, Type 2 -1	2.7	3	T1a	M0
Papillary RCC, Type 2-2	5	2	T1a	M0
Clear Cell RCC -1	8	3	T3a	M0
Clear Cell RCC - 2	10.8	4	T3a	M0
Clear Cell RCC - 3	11	4	T4	M0
Clear Cell RCC - 4	8.2	3	T3a	M0
Clear Cell RCC - 5	8.6	2	T3a	M0
Clear Cell RCC - 6	7.5	3	T2a	M0
Clear Cell RCC - 7	17	1	T2b	M0
Chromophobe RCC - 1	9	2	T2a	M0
Chromophobe RCC - 2	17.5	3	T3a	M0
Chromophobe RCC - 3	5.5	3	T3a	M0
Renal Oncocytoma - 1	6.7	-	-	-
Renal Oncocytoma - 2	7.3	-	-	-
Renal Oncocytoma - 3	8.5	-	-	-

c

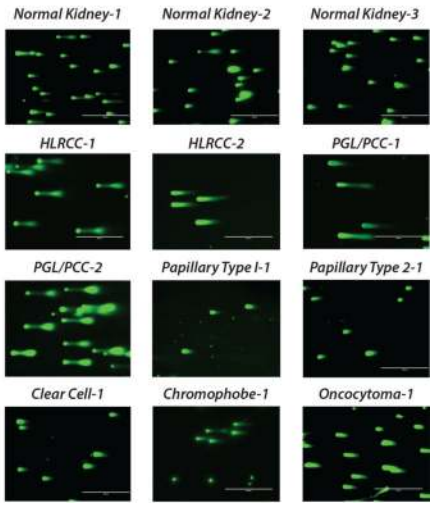

Figure 1. High levels of succinate or fumarate in patient-derived HLRCC and PGL/PCC tumors correlate with elevated DNA double-stand breaks

(a) Liquid chromatography–mass spectrometry (LC/MS) quantification of succinate and fumarate, as indicated, along with quantification of DNA double-strand breaks (DSBs) by the neutral comet assay in a series of human tumor samples and normal tissue specimens, as indicated. For LC/MS n=1; for neutral comet assay, n=3 replicates per clinical sample; bars represent mean +/− SEM. (b) Clinical characteristics of the patient-derived tumor samples studied. (c) Representative images of neutral comet assays as a measure of DNA DSBs performed on the human tumor samples and normal tissues as quantified in panel a. For each clinical sample the assay was repeated 3 independent times.

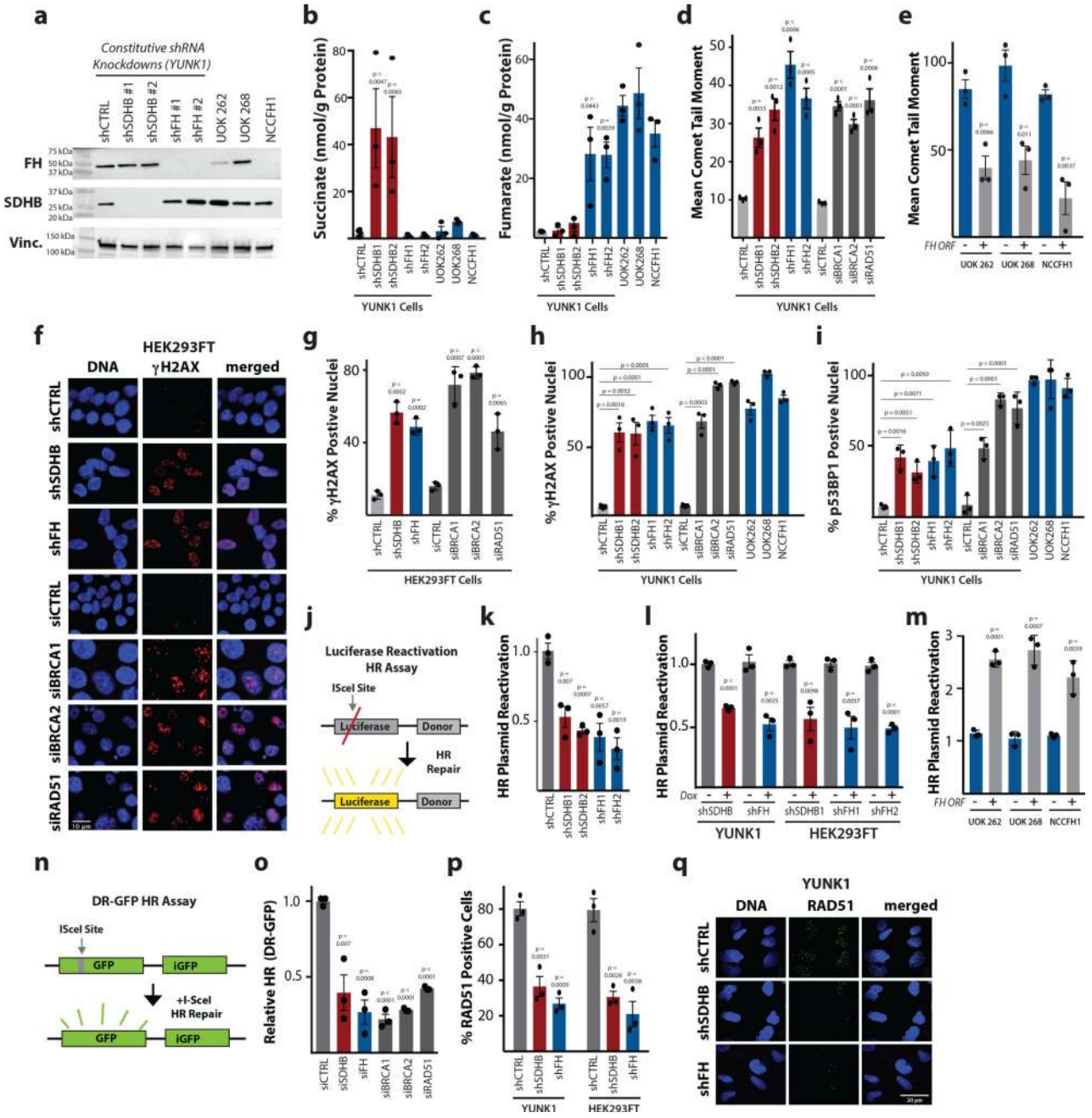

Figure 2. Deficiency in succinate dehydrogenase or fumarate hydratase causes reduced homologous recombination (HR) DNA repair, elevated DNA double-strand breaks, and increased DNA damage response foci

(a) Western blot analysis of SDHB and FH expression in constitutive shRNA models of SDHB or FH knockdown in YUNK1 cells, as well as in the patient-derived, FH-deficient HLRCC cell lines, UOK 262 (FH −/−), UOK 268 (FH p.His192Asp) and NCCFH1 (FH−/−) This analysis was independently performed 3 times with similar results, and images were cropped around the known molecular weight of the band of interest. Full blots appear in supplementary Figure 6. (b and c) LC/MS quantification of (b) succinate and (c) fumarate after SDHB and FH knockdown in YUNK1 cells and HLRCC cell lines. (d) Quantification

of neutral comet assay in YUNK1 cells with or without SDHB or FH knockdown compared to knockdown of the core HR factors, BRCA1, BRCA2, and RAD51. (e) Quantification of neutral comet assay performed in HLRCC patient-derived cell lines with (+FH) or without *FH* plasmid complementation. (f) Representative images and (g) quantification of γH2AX foci staining performed in HEK293FT cells with or without knockdown of the indicated factors. Quantification of (h) γH2AX and (i) p53BP1 foci in YUNK1 shRNA models of SDHB and FH knockdown, in HLRCC cell lines (UOK 262, UOK 268, and NCCFH19), and upon siRNA suppression of core HR factors in YUNK1 cells. (j) Luciferase-based plasmid reactivation assay to report HR. (k–m) Quantification of luciferase reactivation by HR in (k) YUNK1 cells with shRNAs suppressing SDHB and FH, (l) in doxycycline-inducible shRNAs targeting SDHB and FH in YUNK1 and HEK293FT cells, and (m) in patient-derived HLRCC cell lines transiently transfected or not with a plasmid expressing *FH* for complementation of the *FH* deficiency. (n) DR-GFP assay to report HR in U2OS cells. (o) Quantification of DR-GFP HR assay after transfection of U2OS cells with siRNAs targeting SDHB or FH as well as core HR factors. (p) Quantification of RAD51 foci formation upon 2 Gy IR treatment of YUNK1 and HEK293FT cells with or without shRNA suppression of SDHB or FH. (q) Representative images of RAD51 foci formation upon 2 Gy IR in YUNK1 cells with or without shRNA suppression of SDHB or FH. This analysis was repeated 3 times with quantification shown in panel p. For b, c, d, e, g, h, i, k, l, m, o and p statistical analyses were by two-sided t-test (df=4); bars represent mean of 3 independent experiments +/− SEM.

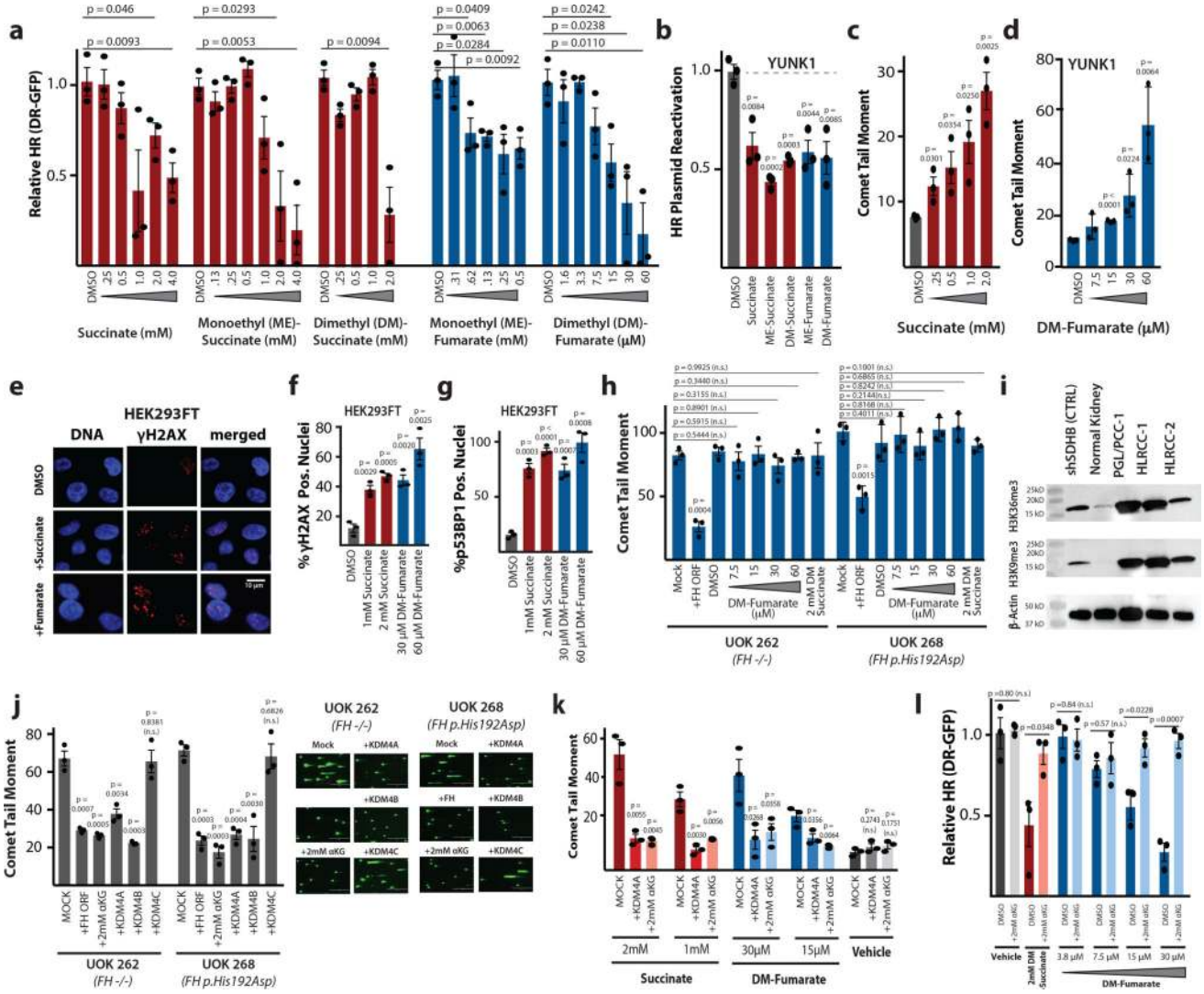

Figure 3. High levels of succinate and fumarate suppress homologous recombination and induce elevated DNA double-strand breaks in a pathway mediated by the lysine demethylases, KDM4A and KDM4B

(a) Quantification of U2OS DR-GFP HR assay after 24 h treatment with indicated doses of indicated metabolites. (b) Quantification of luciferase reactivation by HR in YUNK1 cells after 24 h treatment with 2 mM succinate, 2 mM monoethyl-succinate, 2 mM dimethyl-succinate, 1 mM dimethyl-fumarate, or 60 μM dimethyl-fumarate. (c-d) Quantification of neutral comet assay performed in YUNK1 cells after 24h treatment with indicated doses of (c) dimethyl-fumarate and (d) succinate. (e) Representative images and corresponding quantification of HEK293FT cells treated with 2 mM succinate (Succ) or 30uM dimethyl-fumarate (Fum) for 24h prior to immune fluorescence staining for γH2AX or DAPI staining for DNA. This analysis was independently performed 3 times with similar results and quantification is shown in f. (f) Quantification of (f) γH2AX and (g) p53BP1 foci in HEK293FT cells treated with indicated doses of metabolites. (h) Quantification of the neutral comet assay performed in UOK 262 and UOK 268 HLRCC cell lines with or without transient transfection with an FH expression construct or after 24 h treatment with the

indicated doses of succinate or dimethyl-fumarate or with DMSO control. (i) Western blot analysis of histone 3 lysine 36 trimethylation (H3K36me3) and histone 3 lysine 9 trimethylation (H3K9me3) levels in normal kidney and in patient-derived samples of PGL/PCC and HLRCC tumors, with numbering of respective samples corresponding to Fig. 1. Actin is used as a loading control and YUNK shSDHB1 is included as a control. This analysis was independently performed 2 times with similar results, and images were cropped around the known molecular weight of the band of interest. Full blots appear in supplementary Figure 6. (j) Quantification and representative images of neutral comet assays performed in HLRCC cell lines, UOK 262 and UOK 268, with or without transfection with expression constructs for FH, KDM4A, KDM4B or KDM4C or treatment with 2mM dimethyl-α-ketoglutarate (αKG). (k) Quantification of neutral comet assay performed in YUNK1 cells treated for 24 h with the indicated doses of metabolites, with or without concurrent transfection with KDM4A expression constructs or with 2 mM dimethyl-α-ketoglutarate treatment. (l) DR-GFP assay after treatment with the indicated doses of dimethyl-succinate, dimethyl-fumarate and/or dimethyl-α-ketoglutarate. For a,b,c,d,f,g,h,j,k and l statistical analyses were by two-sided t-test (df=4); bars represent mean +/− SEM of 3 independent experiments.

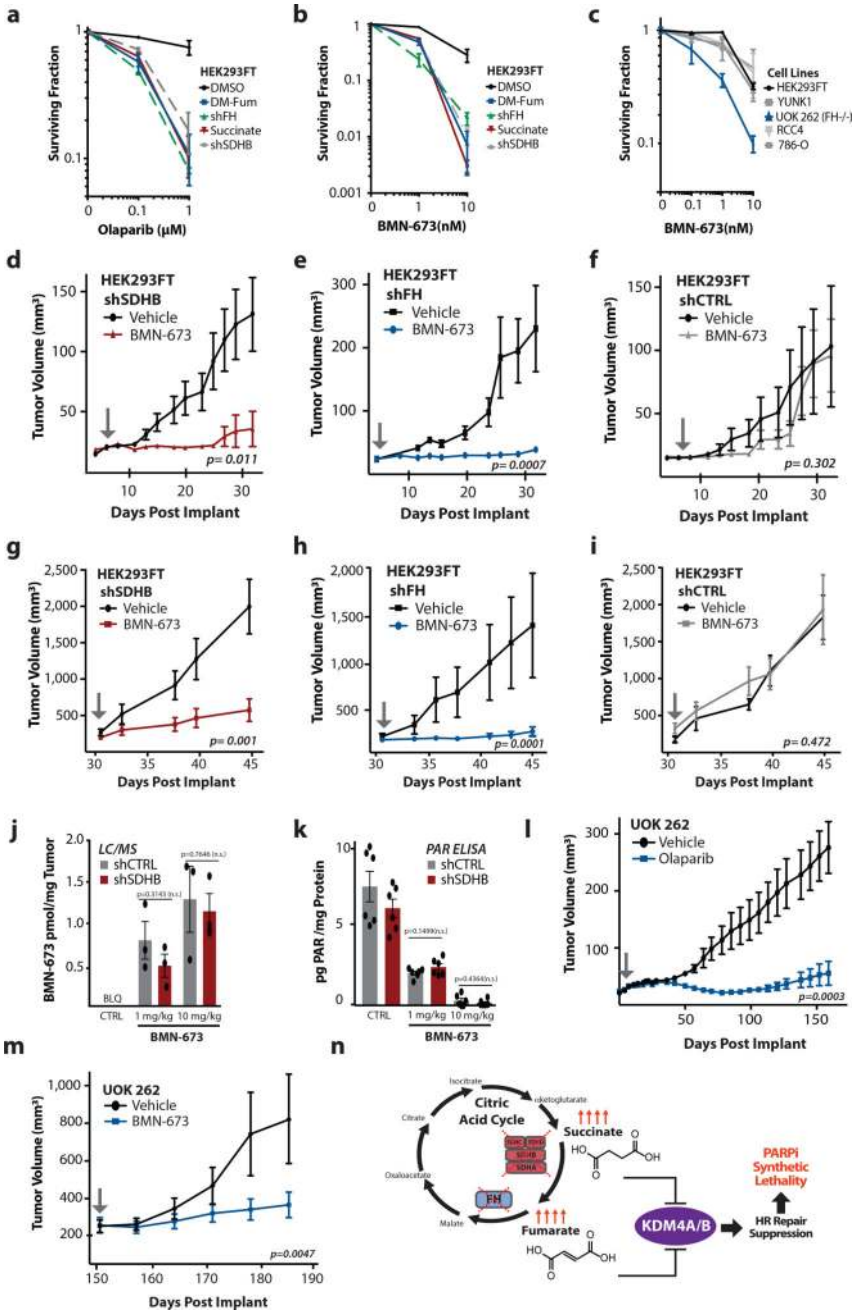

Figure 4. SDHB or FH deficiency confers PARP inhibitor sensitivity on human cells in culture and human tumor xenografts in mice

(a–b) Clonogenic survival assays in response to the PARP inhibitors (a) Olaparib and (b) BMN-673 in HEK293FT cells with or without knockdown of SDHB or FH, or with or without treatment with 2 mM succinate or 60 μM dimethyl-fumarate, as indicated. (c) Clonogenic survival assays in response to the indicated doses of BMN-673 in cell lines of renal origin. For a,b, and c, dots represent mean of 3 independent replicates +/− SEM. (d–f) Tumor growth delay assay in (d) shSDHB-expressing ($F(1, 234) = 40.61$), (e) shFH-expressing ($F(1, 144) = 15.71$) and (f) non-targeted control shCTRL-expressing ($F(1, 234) = 0.27$) HEK293FT tumor xenografts in nude mice treated with BMN-673 or vehicle

control. (g–i) Tumor growth delay assay in (g) shSDHB-expressing (ANOVA F (1, 90) = 28.58), (h) shFH-expressing (ANOVA F (1, 126) = 20.49), and (i) non-targeted control shCTRL (ANOVA F (1, 90) = 4.23)-expressing HEK293FT xenograft tumors treated with BMN-673 or vehicle control. Treatment was initiated when tumors had reached an average size of 95–150 mm^3 (arrow). There were 10 animals per group for d, e, and f and 10 animals per groups for g, h, and I each harboring a single tumor. (j) LC/MS quantification of BMN-673 accumulation in HEK293FT shSDHB and shRNA control xenograft tumors (approximate size at treatment of 80 mm^3) 24 h after treatment of mice with a single dose of BMN-673, as indicated, bars represent mean +/− SEM, n=3. Statistical analysis by two-sided t-test, df=4. (k) Quantification by ELISA of total poly-ADP-ribose (PAR) levels in HEK293FT shSDHB and shRNA control xenograft tumors 24 h after treatment with a single dose of BMN-673, bars represent mean +/− SEM, n=6, statistical analysis by two-sided t-test, df=10. (l) Tumor growth delay assay in patient-derived, HLRCC UOK 262 xenograft tumors in nude mice treated with Olaparib or vehicle control starting 4 days after implantation (arrow) (ANOVA F (1, 532)= 185.2). (m) Tumor growth delay assay in patient-derived, HLRCC UOK 262 xenograft tumors in nude mice treated with BMN-673 or vehicle control starting once tumors reached an average size of 250 mm^3 (ANOVA F (1, 48) = 8.79). For l, 10 mice per group and for m, 6 mice per group. For all tumor growth delay curves shown in d, e, f, g, h, I, l, and m dots represent mean +/− SEM, and the p values were determined by ANOVA. For d,e,f,g,h,i,l,m arrows represent treatment start. (n) Proposed model of succinate- and fumarate-induced HR suppression via inhibition of KDM4A/B leading to synthetic lethality with PARP inhibitors.